Pro-L*: A probabilistic L* mapping tool for ground observations in the radiation belts

Rhys L Thompson[1] | S. K. Morley[2] | C. E. J. Watt[3] | S. N. Bentley[3] | P. D. Williams[3]

University of Reading

Affiliations

- [1]Department of Mathematics and Statistics, University of Reading, UK
- [2]Los Alamos National Laboratory, Los Alamos, USA
- [3]Department of Meteorology, University of Reading, UK

Contact : r.l.thompson@pgr.reading.ac.uk

Pro-L* data is freely available at http://dx.doi.org/10.17864/1947.222

Summary

Mapping ground observations to an L* in space has significant value since the extensive coverage of ground instruments on Earth can be extended into space. Pro-L* allows the combination of magnetic field models (which can significantly disagree on mapped L* for a single ground location) to form L* probability distributions that can better inform location in radiation belt modelling.

Introduction

The third adiabatic invariant, ϕ, measures the magnetic flux through drift contours of azimuthally drifting energetic particles trapped in the Earth's magnetic field

$$\Phi = \int \boldsymbol{B} \cdot d\boldsymbol{S}$$

The Roederer (1970) L*, a label for a particular drift shell whose equatorial point would be at an approximate distance from the Earth's centre if magnetic field lines were relaxed to a dipole, is often used instead of Φ in adiabatic invariant space

$$L^* = 2\pi B_E {R_E}^2/\Phi$$

Ground observations are frequently used in modelling for space weather related processes. Global magnetic field models allow for ground locations to be mapped along field lines to a location in space and transformed into L*, provided they are on closed field lines. Magnetic field models can significantly disagree on mapped L* for a single ground location.

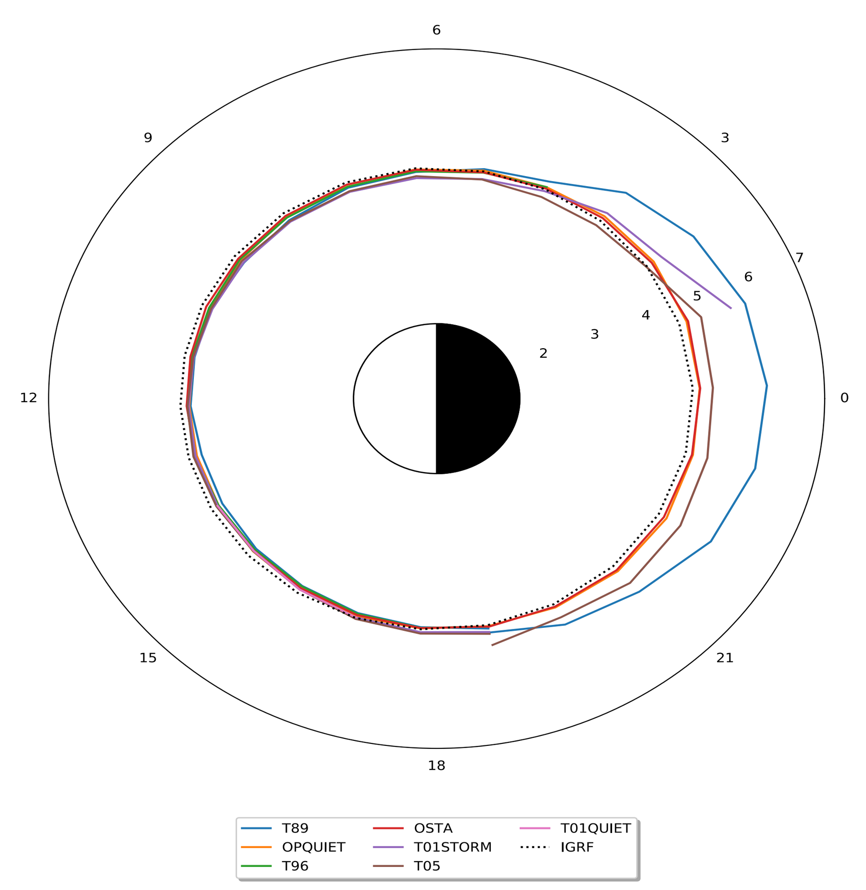

Figure 1: Mapped L trajectories for a single ground location over one day, for a number of global magnetic field models (including the IGRF with no external field applied)*

Probabilistic L* (Pro-L*)

We have created Pro-L*, a probabilistic L* mapping tool for ground observations in space weather modelling. Pro-L* includes 11 years of mapped L* values using 7 popular magnetic field models, over a 16 x 24 grid (magnetic latitude x magnetic longitude, latitude uniform in dipole L) in the Northern Hemisphere. At each mapped equatorial location the following variables are also stored:

- McIlwain L
- Minimum **B**-field
- Cartesian location

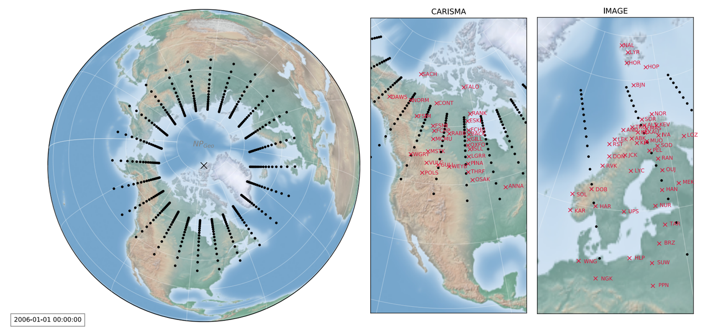

Figure 2: A snapshot in time of (left) the Pro-L spatial domain in AACGM coordinates projected down onto the magnetic North Pole (x), as well as onto two popular magnetometer arrays: CARISMA (centre) and IMAGE (right).*

Global L* statistics for both individual magnetic field models and probabilistic combinations have been tabulated with uncertainties quantified for easy implementation in modelling (please contact if interested in using). Effective interpolation to user-specific ground instruments has been explored.

Code	Model
OPQUIET	Olson and Pfitzer (1974)
T89	Tsyganenko (1989)
T96	Tsyganenko (1996)
OSTA	Ostapenko and Maltsev (1997)
T01QUIET	Tsyganenko (2002)
T01STORM	Tsyganenko et al. (2003)
T05	Tsyganenko and Sitnov (2005)

Table 1: External magnetic field models used in Pro-L for variable calculations*

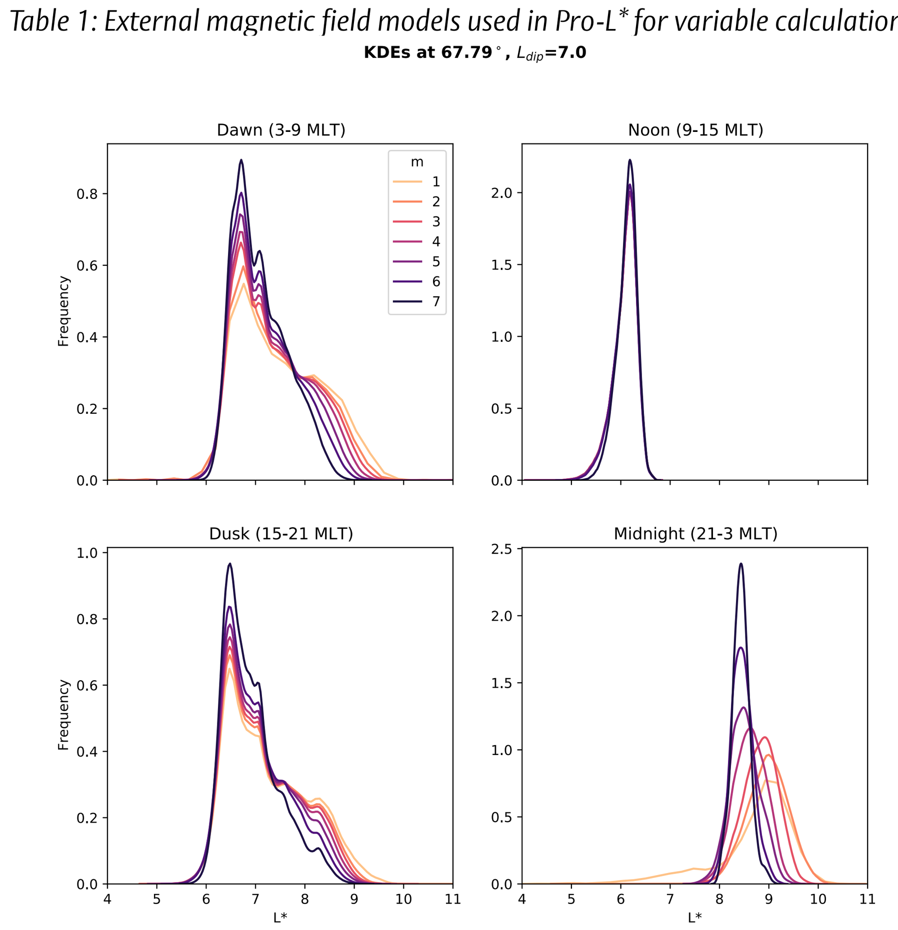

Figure 3: Kernel density estimates (KDEs) of global probabilistic L models at 67.79° magnetic latitude separated into MLT sector. The KDEs are shown as a function of the number of magnetic field models returning an L* value, m.*

Model statistics

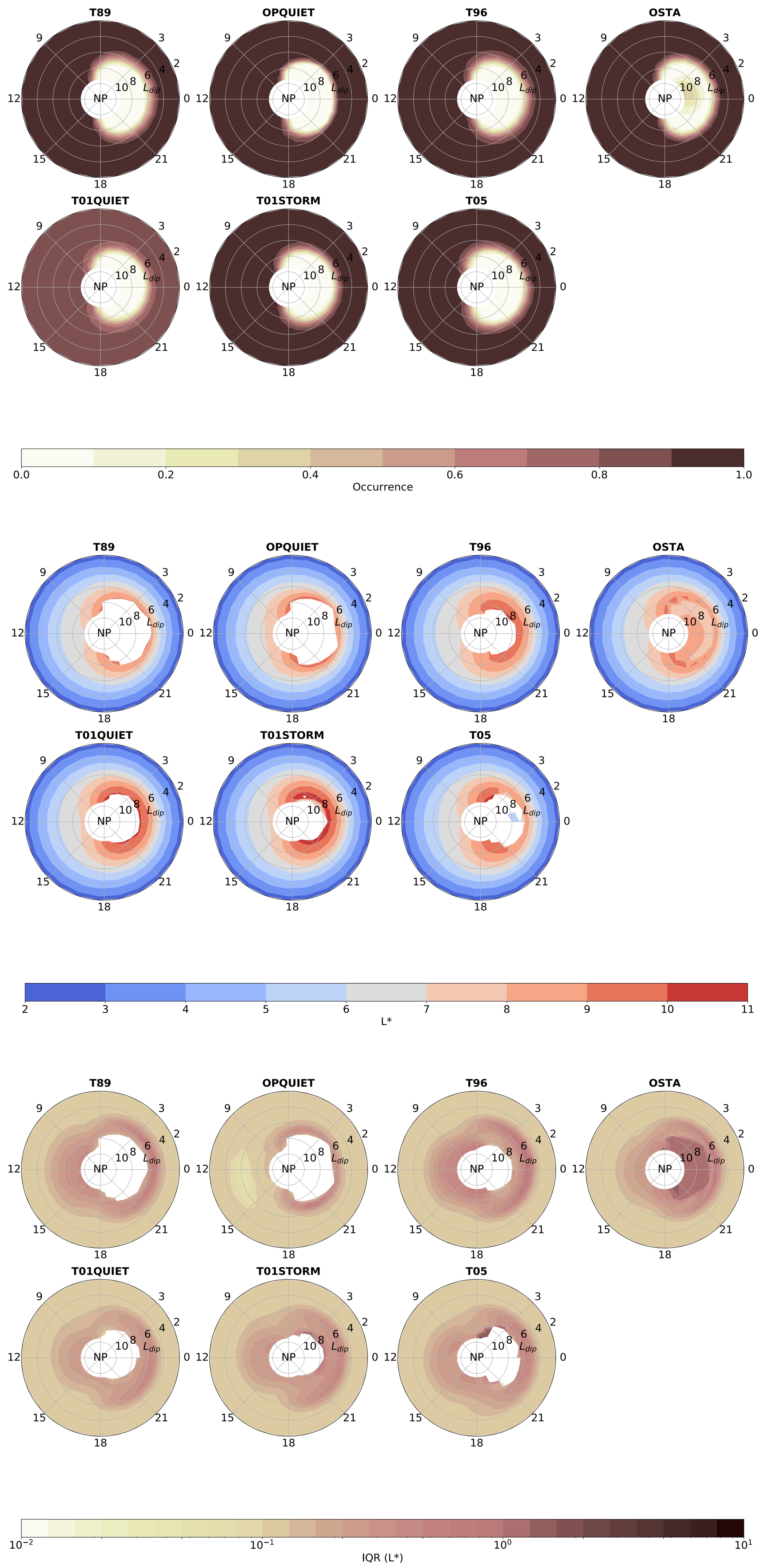

Figure 4: Global occurrence (TOP), median (MIDDLE) and interquartile range (IQR) (BOTTOM) maps for a defined L shown for each magnetic field model. The maps are displayed in MLT and magnetic latitude, projected onto the magnetic North Pole with the Sun to the left. Magnetic latitudes have been transformed into their dipole equivalent to ensure a uniform distance between radial bins. The occurrence values were calculated as the ratio between the number of L* values returned to the total number of observations (L* defined and undefined) in each bin.*

References

1. Roederer (1970), *Dynamics of geomagnetically trapped radiation, Springer-Verlag Berlin*
2. Tsyganenko (1989), *Planetary and Space Science*
3. Olson and Pfitzer (1974), Tsyganenko (1996, 2002), Ostapenko and Maltsev (1974), Tsyganenko and Sitnov (2005), *Journal of Geophysical Research: Space Physics*

Acknowledgements

- This work was supported by the Engineering and Physical Sciences Research Council (EPSRC) grant EP/L016613/1

Test case: Storm dropout

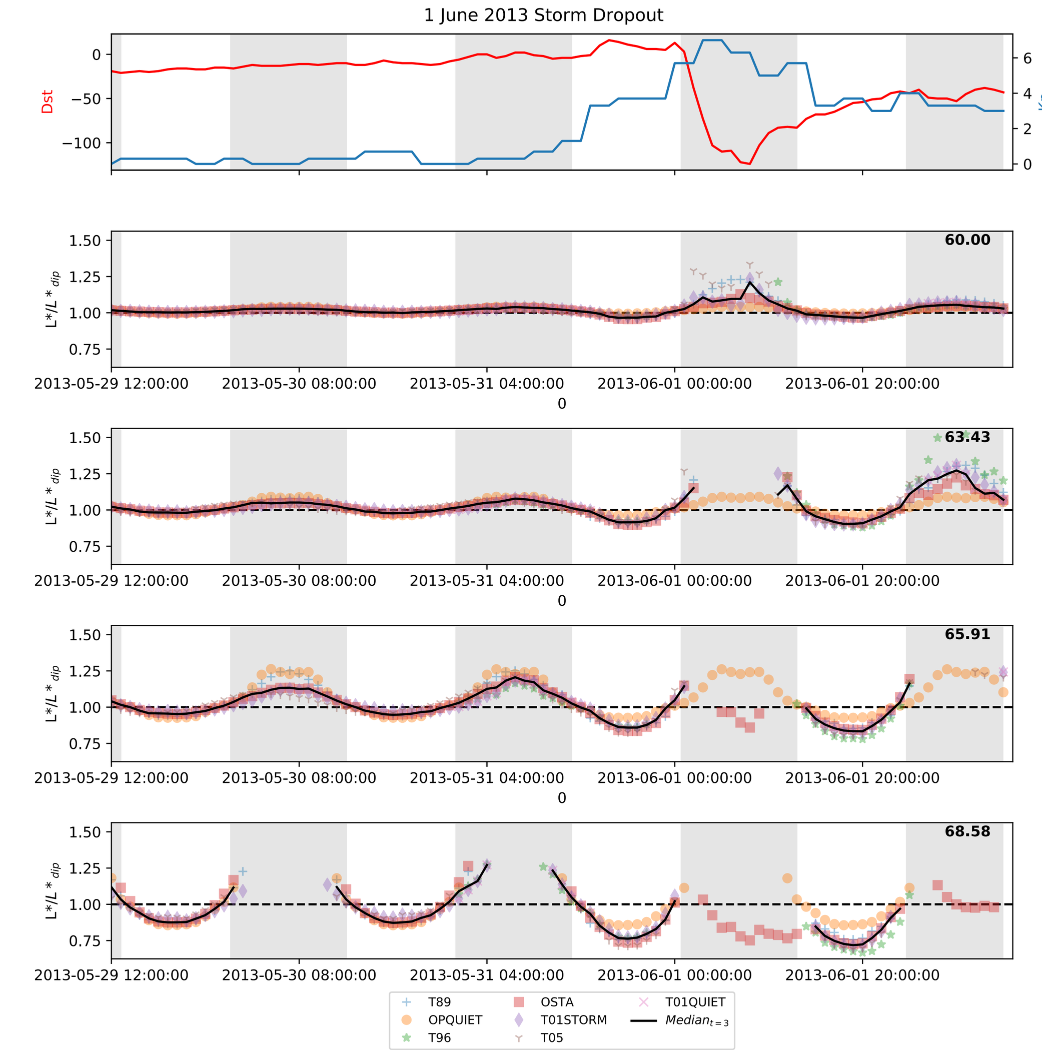

Figure 5: The response of L during the Children's Day storm dropout on 1 June 2013 for each magnetic field model, at a selection of magnetic latitudes (in the vicinity of CARISMA, magnetic longitude 330°). The median L* is also given provided that at least 3 magnetic field models return an L* value. All returned L* are normalised by their respective constant dipole approximation for comparison of latitudes on the same scale. The Dst and Kp indices are also provided over the given time period. Shaded bars indicate times where observed values are on the nightside.*

Grid interpolation

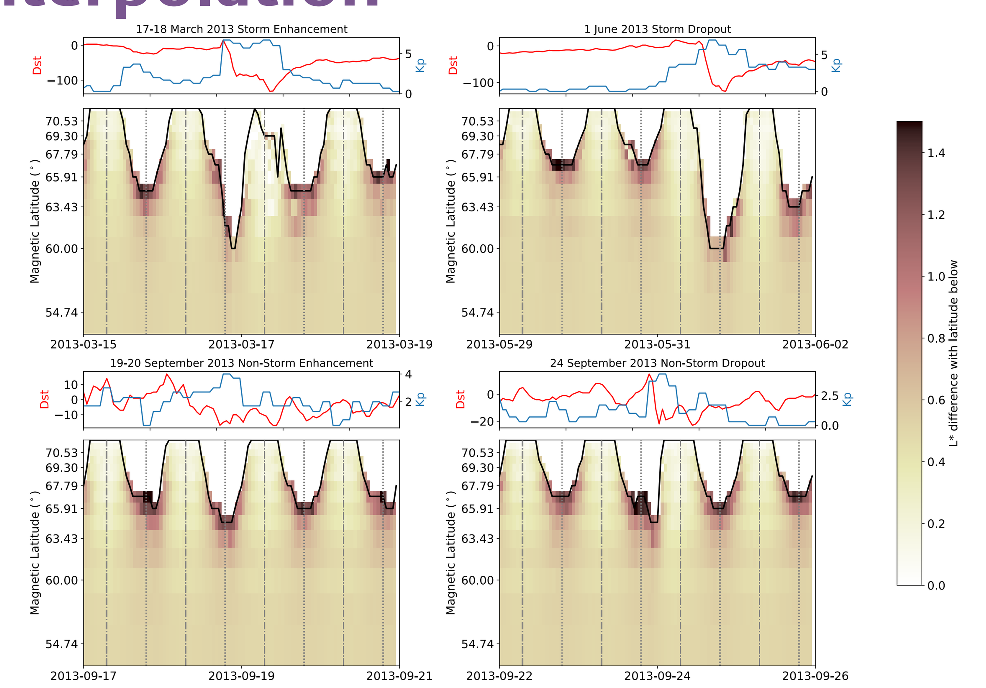

Figure 6: The latitudinal change in L (northwards), where L* is the median of all magnetic field outputs provided that at least 3 magnetic field models to provide an L* output (else L* is assumed to be undefined), shown for the 4 2013 GEM challenge events at 300° magnetic longitude. The boundary for monotonic increases is illustrated with a black line. Vertical lines for midday (dash-dot) and midnight (dotted) are also shown.*

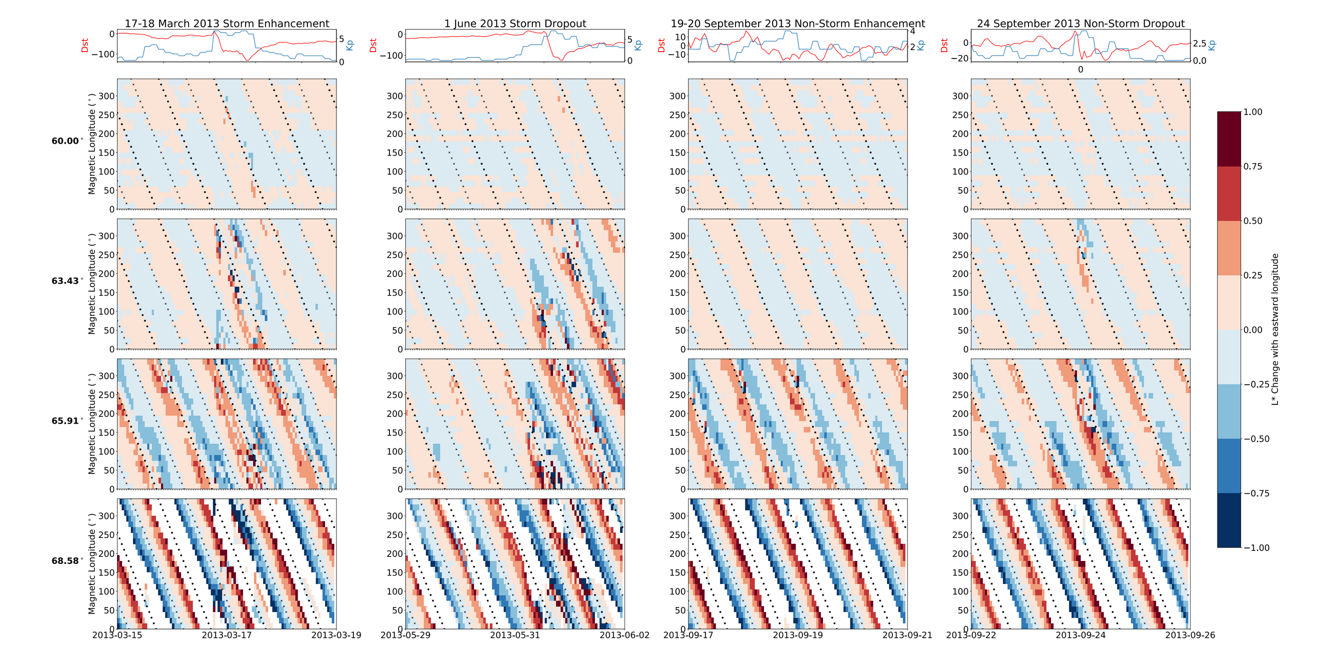

Figure 7: The longitudinal change in L (eastwards), where L* is the median of all magnetic field outputs provided that at least 3 magnetic field models to provide an L* output (else L* is assumed to be undefined), shown for the 4 2013 GEM challenge events (columns) and a selection of magnetic latitudes (rows). Markers for midday (+) and midnight (x) are also shown.*